Carbon xxx (2017) xxx-xxx

Contents lists available at ScienceDirect

Carbon

journal homepage: www.elsevier.com

Rationalizing and reconciling energy gaps and quantum confinement in narrow atomically precise armchair graphene nanoribbons

Aristides D. Zdetsis [a, b, *], E.N. Economou [b]

[a] Molecular Engineering Laboratory, Department of Physics, University of Patras, Patras, 26500 GR, Greece
[b] Institute of Electronic Structure and Laser, Foundation for Research &Technology Hellas, Vassilika Vouton, P.O. Box 1385, Heraklion, Crete, GR-71110, Greece

ARTICLE INFO

Article history:
Received 8 August 2016
Received in revised form 30 January 2017
Accepted 2 February 2017
Available online xxx

ABSTRACT

Recent advances in bottom-up production of atomically precise armchair graphene nanoribbons (AGNRs) and their structural and electronic characterization through scanning tunneling microscopy (STM) and spectroscopy (STS) present an opportunity and a challenge for their interpretation and inter-correlation, especially in view of several seemingly conflicting results for their electron distribution and gap size, sometimes by more than 300%. Such large discrepancies, which threaten to undermine the extraordinary achievements of their synthesis, are threefold: Experiment vs. theory; experiment vs. experiment; and theory vs. theory. Here we illustrate that by using many-body corrections through time-dependent (TD) density functional theory (DFT), and proper identification of the STS gap, we can reproduce all known, and predict new as yet unknown, experimental data for such AGNRs. Furthermore, we can rationalize and suggest ways to reconcile practically all known discrepancies. We demonstrate that besides the width measured by the number N of carbon atoms across, the length and the length-variation of the gap properties, which reveal a semiconductor-metal transition, is an important factor which is usually overlooked in the literature. This, together with inherent problems of DFT for accurate gap determination, on top of experimental STS difficulties, are the main sources of such discrepancies.

1. Introduction

Graphene based materials such as Graphene Nanoribbons (GNRs) and various forms of nanographens have been developed to alleviate the main drawback of zero band-gap of pristine graphene for nanoelectronics applications [1,2]. However, the usual top down methods of GNR fabrication do not allow the structural and electronic precision required for the fine tuning of their desired properties. In fact, GNRs, together with many other carbon based nanomaterials, with the exception of fullerenes, should not be considered as structurally pure materials [2]. This is because they cannot be separated or refined into pure structural forms [2]. Nevertheless, recent extraordinary developments in Graphene (carbon) synthetic Chemistry have allowed the Bottom-up fabrication of atomically precise GNRs using molecular precursors, and even more important, their complete structural and electronic characterization using scanning tunneling microscopy (STM) and spectroscopy (STS) [1–9]. For a given edge morphology (zigzag or armchair), the (only) critical parameter through which GNRs are classified and identified is considered (up to now) to be their width, which for armchair GNRs (AGNRs) as the ones in the present study, is defined by the number of carbon atoms across their physical width (or the number of carbon-carbon dimer lines making up their width).

The synthesis (and characterization) of atomically precise AGNRs have paved the road for novel technological and scientific developments of graphene based nanomaterials. However, as it happens with most frontier works in their initial breakthrough stages, there exist several ambiguities and discrepancies for their most important characteristics, i.e. the band edges. In particular, the most controversial quantity for the band edges is the magnitude of their energy separation (gap), as determined by STS [3,4]; followed by their "morphology", as shown by the electron distribution/localization in the highest occupied and lowest unoccupied molecular orbitals (HOMO and LUMO, respectively) [6]. In some cases the quoted differences (discrepancies) for the gap size of the "same" AGNR appear to be huge (more than 300%); thus hindering the real understanding, rationalization, and inter-correlation of the results, and consequently, the further development and design of more novel structures. Some striking discrepancies about band gap are summarized in Table 1, in which we can see that the claimed measured gap of the N = 5 GNR in one work [4] is about 0.1 eV, and in another [3] 2.8 eV. The same is true in comparing different theoretical works or experimental and theoretical works for other AGNRs of widths N = 7, 9, 11, and 13.

The second type of discrepancy, about the morphology of HOMO and LUMO (and the "nearby" frontier orbitals) is shown in Fig. 1. In this figure, which is based on our own calculations, contrary to earlier theoretical predictions [12–14] and some experimental STS results [4] showing a spatially extended nature of the HOMO and LUMO orbitals, we can see HOMOs and LUMOs which are well lo-

* Corresponding author. Molecular Engineering Laboratory, Department of Physics, University of Patras, Patras, 26500 GR, Greece.
Email address: zdetsis@upatras.gr (A.D. Zdetsis)

http://dx.doi.org/10.1016/j.carbon.2017.02.006
0008-6223/

Table 1
Measured (Refs. [3–6]) and Calculated (Refs. [10,11]) band gaps (in eV) for the N = 5, 7, 9, 11, and 13 AGNRs.

AGNR	exp Refs. [1,4–6]	exp Refs. [2,3,6,7]	This work TDDFT/PBE0	LDA Ref. [11]	LDA + GW Yang et al. [10]
N = 5	0.1[a]	2.8	0.1	0.4	1.7
N = 7	2.3	2.5	2.3	1.6	3.8
N = 9	–	–	1.6	0.7	2.0
N = 11	–	–	0.45	0.2	0.9
N = 13	1.4	–	1.4	0.8	2.4

[a] This value is consistent only for the very long (longer than 10 nm) AGNRs.

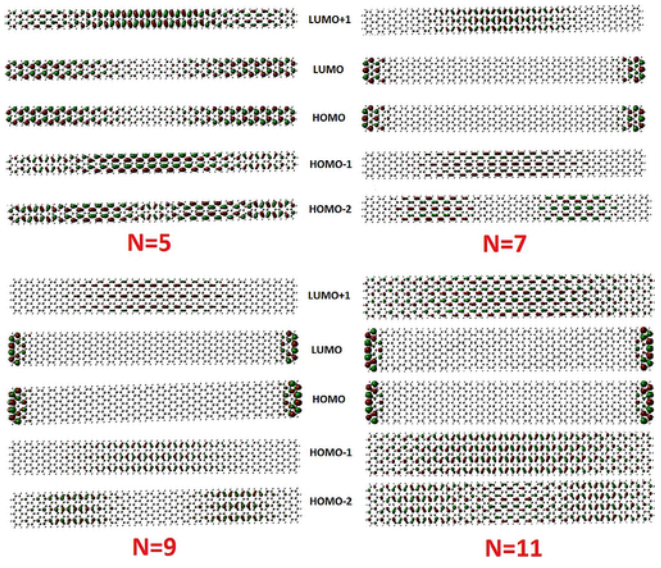

Fig. 1. Frontier orbitals (HOMO-2, HOMO-1, HOMO, LUMO, LUMO+1, LUMO+2) of selected narrow GNRs of widths N = 5, 7, 9, and 11 of about 6.75 Å, 9.2 Å, 11.7 Å, and 14.1 Å, respectively; and common length of about 103.6 Å (10.4 nm). The quoted lengths include the surface hydrogens and correspond to fully relaxed structures. (A colour version of this figure can be viewed online.)

calized at the zigzag edges of the AGNRs, in full agreement with the results of other experimental works [6,8].

So then, what is correct and what is incorrect? Or who is right, and who is wrong? As it happens in such cases [14,15] there is no clear yes-or- not answer, because most of the times we are not comparing identical objects and/or states (data or theories of "different validity"), or we are missing some critical detail(s) and parameters. This is analogous to the early years of silicon nanocrystal research, for the critical gap-versus -size results, with many different mutually conflicting theoretical and experimental results for the same size nanocrystal [14,15]. A similar situation involving both theory and experiment was the question of the real structure of the "magic" the Si_6 cluster [16].

The "solution" in those cases, according to our opinion and earlier experience [14–16], is the application of a suitable reliable, well tested, and efficient theoretical framework to describe all relevant experimental results in a simple (as possible), uniform and unbiased way for all structures (small and large), and in a reasonable (computing) time. Such a scheme can be also used as a "yard stick" for existing and future data [15].

In the present communication, we have adopted a reliable and efficient atomistic approach (in real space) based on density functional theory (DFT) and time-dependent DFT (TDDFT), with the powerful hybrid functional PBE0[17]. An added advantage of such approach and such techniques is that they are well tested and widely spread, thus facilitating the comparison and testing by others. In our approach, we have considered free standing GNRs, which is a common assumption in most works (experimental and theoretical) in analysing and rationalizing their data (as in Table 1 and Fig. 1). This is based on the conclusions of Varykhalov et al. [8], in agreement with the analysis of Zhang et al. [3] and others [4], which suggest that the substrate, Au(111), does not have a significant influence on the overall electronic structure of GNRs, although there is a work with opposing views [5] attributing the failure of the theoretical predictions to substrate (charge screening) effects. Since, as will be shown below, we can fully interpret the current experimental data (and most of the inconsistencies, including the varying morphology of HOMOs and LUMOs) without invoking any substrate corrections, we adopt here consistently the simplest and more common view of free standing GNRs. We illustrate, however, the validity of this assumption by invoking a simple and transparent example, considering the N = 5 "short" AGNR consisting of three perylene monomers. We show that for such AGNR, the overall bandgap renormalization should be only 0.13 eV (around 8%), very small indeed compared to the magnitude of the errors from other sources. We believe that the most important features for the correct analysis of the STS data for such AGNRs (in the framework of quantum confinement) is the influence of their finite length (which is a "hidden variable" in most works), and the correct identification of the STS gap in the (many-body, TDDFT) excitation spectrum.

2. Results and discussion

2.1. General comparisons

Before we embark in the description and discussion of our results for each one of the five AGNRs included in Table 1, we should establish the validity and power of our approach by applying and comparing our methodology to some unbiased, independent, but relevant experimental (and theoretical) results. The experimental (and theoretical) results of Halasinski et al. [18] for the electronic absorption spectra of perylene ($C_{20}H_{12}$), terrylene ($C_{30}H_{16}$), and quaterrylene ($C_{40}H_{20}$) constitute the ideal reference data for such tests, shown in Table 2, since they are all based in perylene, as the synthesized AGNRs of Kimouche et al. [4], which in a sense can be seen as "perylene polymers". After all, about 35% of their produced AGNRs is quaterrylene ($C_{40}H_{20}$), consisting of two perylene monomers, according to Fig. 1 in their supporting information. From the same figure, we can also see that (3) and (5) AGNRs correspond to about 30% and 7%, respectively of the produced AGNRs. In the same table, we include for comparison our present results for the shortest, but most abundant (if we neglect the one and two perylene monomers) N = 5 AGNR (3) consisting of three perylene monomers. The excitation energies in Table 2 correspond to the "optical gap", theoretically determined by TDDFT, and experimentally obtained by the lowest allowed frequency in the excitation (here absorption) spectrum. HOMO-LUMO gaps are the "one particle" energy gaps obtained theoretically (here by DFT) by the difference between the energy eigenvalues of the highest occupied (HOMO) and the lowest unoccupied (LUMO) molecular orbitals. The difference of the optical gap from the HOMO-LUMO (in fact LUMO-HOMO) gap defines the quasiparticle binding energy. As we can see in Table 2, our results are in excellent agreement with experiment. The results for the non-hybrid LDA-like PBE functional have the largest discrepancies of the three, especially for the HOMO-LUMO gaps which are strongly underestimated. This is very important since Kimouche et al. [4] have used this functional in their combined theoretical and experimental analysis of their STS data, and this probably the reason for their gap underes-

Table 2
Comparison of the theoretical TDDFT methods (using PBE0, PBE, and B3LYP exchange and correlation functionals) with experiment (Ref. [18]), and with each other for Perylene, Terrylene and Quaterrylene, consisting of one (1); one and a half (1.5); and two (2) perylene monomers; together with our theoretical predictions for the shortest N = 5 AGNR, comprised of three (3) perylene monomers.

Methods	Perylene ($C_{20}H_{12}$) (1)	Terrylene ($C_{30}H_{16}$) (1.5)	Quaterrylene ($C_{40}H_{20}$) (2)	6-AGNR ($C_{60}H_{28}$) (3)
Experiment Ref. [18]				
Excitation Energy	2.96 eV	2.35 eV	2.04 eV	**(1.55 eV)**[a]
This Work PBE0				
Excitation Energy	**2.98 eV**	**2.31 eV**	**1.93 eV**	**1.48 eV**
Oscillator Strength	0.3796	0.7894	1.2764	2.3858
HOMO-LUMO gap	3.30 eV	2.55 eV	2.10 eV	1.56 eV
Calculated PBE				
Excitation Energy	**2.60 eV**	**1.98 eV**	**1.65 eV**	**1.25 eV**
Oscillator Strength	0.2906	0.6357	1.0630	2.0759
HOMO-LUMO gap	1.91 eV	1.30 eV	0.97 eV	0.62 eV
Ref. [18] **B3LYP**				
Excitation Energy	**2.64 eV**	**2.02 eV**	**1.67 eV**	–
Oscillator Strength	0.3088	0.6734	1.0792	

[a] "Projected" value, meaning the "renormalized" value, assuming that the reassignment of the peaks we have suggested here on the basis of the results of Refs. [3,4] is valid. See text.

timation in the shorter AGNRs. Such underestimation of the gap by PBE and LDA (or LDA based) approaches is well known in the literature [14,15]. As a matter of fact, such gap underestimation was also largely responsible for the apparent discrepancies in the gap versus size results of silicon nanocrystals [14,15]. As we can see in Table 2, the corrected TDDFT/PBE gaps are much better, but still considerably underestimated. However, sometimes especially for LDA, the many body correction to increase the underestimated gap could lead to the other end of overshooting, i.e. to gap overestimation. This seems to be the cases for the LDA + GW results, which however correspond to the infinite length nanoribbon(s). On the basis of the excellent performance of our TDDFT/PBE0 calculations, shown in Table 2 (and in several more demanding calculations for graphene and graphene dots and antidots [19,20]), we propose to use our current theoretical results as a "yard stick" for existing and future work in such atomically precise AGNRs, starting with (and paying more attention to) the most controversial narrowest N = 5 AGNR.

2.2. The N = 5 AGNRs

Besides being the most controversial, the N = 5 AGNR is also the only AGNR with STS data at different lengths [4], the shortest of which consists of three (3) perylene monomers, already listed in Table 2, as a natural continuation of the perylene ($C_{20}H_{12}$), terrylene ($C_{30}H_{16}$), and quaterrylene ($C_{40}H_{20}$) for which there are unambiguous (and unbiased) experimental and theoretical data [18]. On the basis of Table 2, the HOMO-LUMO gap according to our results should have been 1.55 eV, which after the simplest TDDFT many body corrections would be around 1.48 eV. This is clearly seen in the excitation spectrum of Fig. 2, which also shows a secondary peak at about 2.9 eV, which could be compared to the 2.8 eV value suggested by Zhang et al. [3] as the actual gap. We can also see, in agreement with

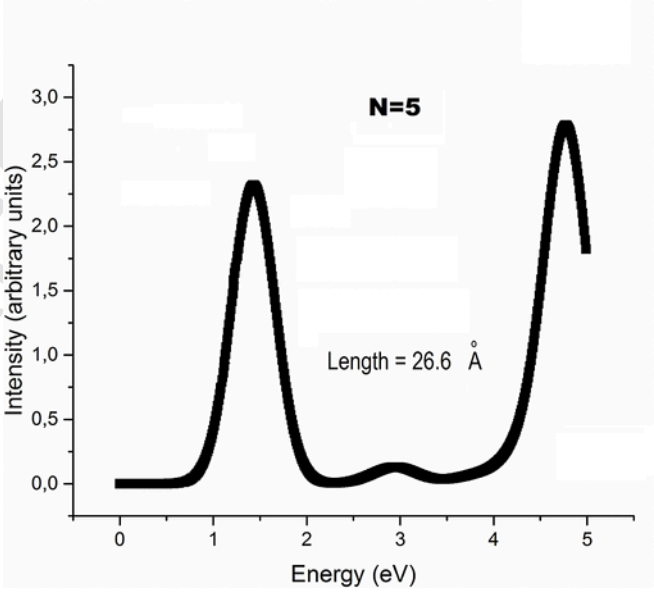

Fig. 2. The many-body TDDFT/PBE0 excitation spectrum of the three (3) Perylene monomer (length of 26.6 Å) N = 5 GNR, of width about 6.75 Å (including end hydrogens).

the conclusions of Kimouche et al. [4] that the many body corrections are small in this case (3). However, Kimouche et al. [4] in their STS analysis (in which they have used the PBE functional) have found a HOMO-LUMO gap of 0.70 eV, which is half of our PBE0 value, but very close to the 0.62 eV value obtained by the PBE functional in Table 2. There could be several reasons for this "discrepancy", some of which we explore below. Nevertheless the "gap", no matter how

we measure it or how we define it (see discussion for the N = 7 AGNR below), according to our results, should be around 1.4–1.5 eV, and not much smaller. Similarly, the gap for the 5 perylene monomer should be around 1 eV, and not 0.22 eV, as have been suggested in Ref. [4]. Of course these values, similarly to the values quoted in the analysis of Kimouche et al. [4], do not include any GNR-substrate interaction and refer to electrically neutral species. As we can see in the results of Halasinski et al. [18], charged species are characterized by much smaller gaps.

To address now (and resolve) the second type of discrepancies about the morphology (electron distribution) at band edges, we have drawn in Fig. 3, the frontier orbitals (together with their orbital energies) for N = 5 AGNRs of various lengths, starting with the shortest (3) of three perylene monomers AGNR. As we can see in this figure, for samples of smaller lengths (less than about 90 Å), such as those studied in detail by Kimouche et al. [4], the HOMOs and LUMOs are indeed extended through the ribbon. On the other hand, for longer AGNRs (>10 nm), a transition to the nature of frontier orbitals seem to occur.

Thus, such (long) N = 5 AGNRs follow the general trend of edge localized HOMOs and LUMOs as observed by several other groups, and as shown in Fig. 1. In this respect no one is wrong, as it was argued earlier. Notice also in Fig. 3 that the HOMO-LUMO energy differences (gaps) are systematically decreasing with increasing length. This is clearly demonstrated in Fig. 4, which shows the length variation of the one-body (HOMO-LUMO) and many-body (TDDFT) gap for N = 5 AGNRs. In full agreement with the results of Kimouche et al. [4], we can see that for long (longer than 10 nm) GNRs the gap approaches the value of 100 meV. We can also observe a rather abrupt drop in both HOMO-LUMO and "optical gap" at about 10 nm which can be interpreted as a pseudo semiconductor/metal transition. Such transition was also suggested by Kimouche et al. [4], but for a much shorter length (about 5 nm).

As we can see in Fig. 4 at this point the exciton "binding" energy (the difference between TDDFT and DFT gaps) changes sign. At this point, as can be verified by comparing Figs. 1 and 3, the nature of the HOMO and LUMO orbitals changes from extended to edge- localized. Thus before this length (10 nm) the band-edges states are extended through the ribbon, whereas at lengths larger than the "critical length" they are mostly localized at the zigzag ribbon edges. Furthermore, we can see a length region between 4 nm and 9 nm (40 Å- 90 Å) in which the TDDFT and DFT gaps almost coincide (the difference is practically zero) before the difference turns negative after the critical length of 9–10 nm. Obviously in this region we have clear one particle (electron) excitations without significant many-body contributions. It should be emphasized that in our study such rather well defined transition has not been observed for the wider (N = 7, 9, 11) AGNRs, as is shown in Fig. 5; and therefore should be related to the very small width (strong lateral confinement) of N = 5.

Nevertheless, the general trend of gap variation with length is the same, from which it is deduced that AGNRs of the same width, but of substantially different lengths could have substantially different gaps, unless of course they are in the region of gap saturation, which occurs after some critical length(s). From Fig. 5 we can see that for the GNRs examined here, with the exception of the very narrow N = 5 GNR, this "critical length" is about 4–6 nm. Length, therefore somehow plays a role of a "hidden variable"; and there is no unique gap, unless we have reached the "saturation point" after some critical length. Obviously, this is one, if not the main, large source of confusion. It becomes also clear from the above picture that the 0.1 eV gap of Kimouche et al. [4] for the N = 5 GNR is "correct" for the long (longer than 10 nm), not for the short (3) and (5) AGNRs.

2.2.1. Some speculative remarks and suggestions

Although it is not our responsibility or our target to pinpoint possible sources of discrepancies in somebody else's (very important and delicate) work, it is however tempting to try to bridge the gap in the literature. In particular, for the (3) and (5) N = 5 AGNRs, on the basis of the assumed reliability of our results (as far as was established here and elsewhere [19,20]) using them as a "yard stick", we attempt to trace the sources of discrepancies in a constructive way to the benefit of future work. This is certainly within the assumptions (and restrictions) of free standing, neutral samples, which are however very common, as was explained earlier. Obviously, there could be alternative interpretations and suggestions.

2.2.1.1. The three perylene monomers (3) AGNR

On the basis of their STS data Kimouche et al. [4] have experimentally identified the HOMO-1 orbital at −1.02 eV, the HOMO at −0.16 eV, LUMO at +0.54 eV and their LUMO+1 at 1.80 eV. These values are not directly comparable to our values, shown in Fig. 2, which are with respect to vacuum (not to the Fermi level). Only the energy differences are meaningful. According to these values the "measured" HOMO-LUMO gap should be 0.70 eV, which appears to be in good agreement with the theoretical HOMO-LUMO gap obtained by the PBE functional, giving apparent confidence in the as-

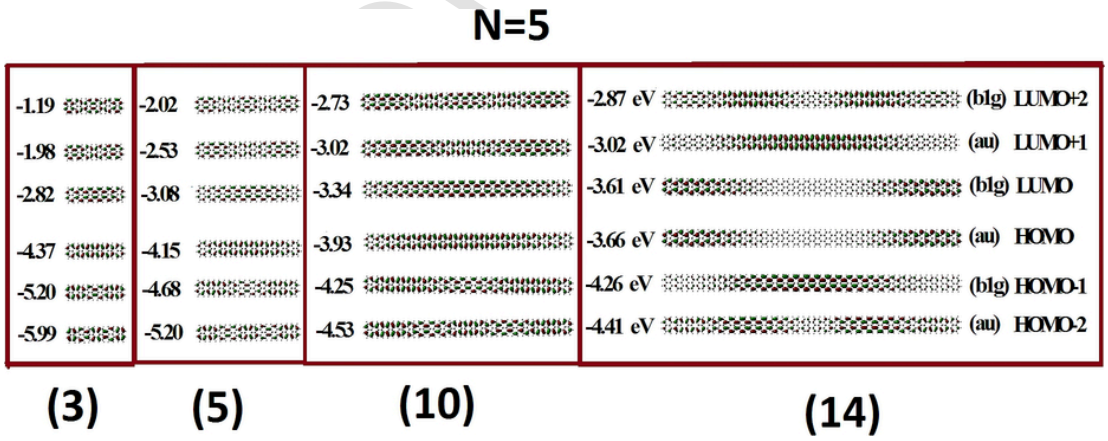

Fig. 3. Frontier orbitals (HOMO-2, HOMO-1, HOMO, LUMO, LUMO+1, LUMO+2) of the N = 5 GNR (of constant width of about 6.75 Å) and various lengths consisting of three (3), five (5), ten (10), and fourteen (14) Perylene monomers with real lengths of 26.6 Å, 43.8 Å, 86.5 Å, and 121.2 Å, respectively. Orbital energies and symmetries are also indicated in the Figure. The above lengths include the edge hydrogen atoms. (A colour version of this figure can be viewed online.)

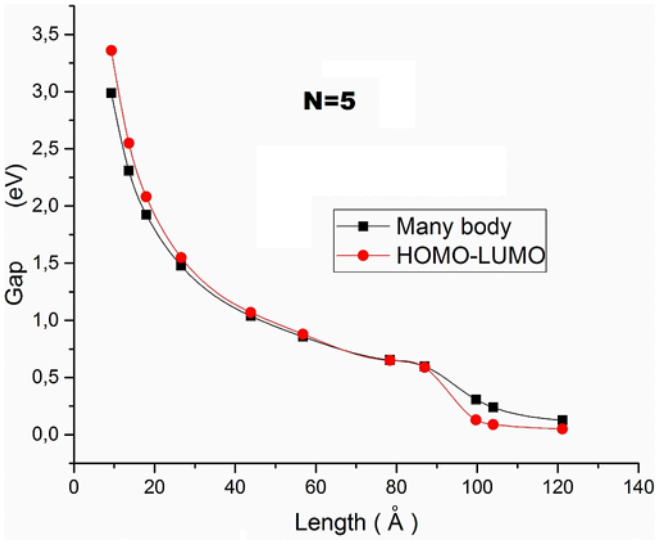

Fig. 4. Length dependence of the one-body HOMO-LUMO (DFT/PBE0), and "many-body" (TDDFT/PBE0) energy gap of the constant width (6.75 Å) N = 5 GNR. (A colour version of this figure can be viewed online.)

signed experimental STS HOMO-LUMO; and thus, leading to the conclusion that no many-body corrections are needed, which is true for the PBE0, as we illustrated earlier (Table 2 and Fig. 4). However, for the PBE functional used by Kimouche et al. [4], the many-body corrections through TDDFT almost double the gap value, as we can see in Table 2. Therefore, using our own results as a "yard stick", we are lead to consider alternative interpretation by matching appropriate energy differences. We found, as can be easily verified, that the assigned by Kimouche et al. [4] (HOMO-1)-LUMO difference is 1.56 eV, practically identical to our PBE0 HOMO-LUMO gap, and in excellent agreement with the 1.48 eV many-body corrected TDDFT/PBE0 gap. Therefore, we are lead to suggest as one, but not the only one, possible way to reconcile the STS data with our results, that the peak at −0.16 eV (initially assigned by Kimouche et al. [4] to HOMO) could be spurious. Then, the real HOMO should be at −1.02 eV (initially assigned to HOMO-1). The LUMO would remain at +0.55 eV (as was originally assigned). Alternatively, we could fix the experimental values of the HOMO-1 and HOMO energies and seek more appropriate LUMO values. We can also see that if one misses the LUMO peak, then the LUMO+1 will be assigned as LUMO and in that case (always according to the results of Ref. [4]) the "assigned" gap would be 1.80 –(-1.02) = 2.82 eV, which is exactly the value obtained by Zhang et al. [3]. According to our results in Table 2, such large gap would be reasonable only for extremely short "AGNRs" of about 1 perylene monomer. Excluding such possibility, we could assume, in line with the suggestion of Kimouche et al. [4], that the real LUMO peak has escape attention and that the LUMO+1 was mistaken as LUMO. This can be also deduced from the results of Zhang et al. [3], who have locate their HOMO at −0.69 eV, but before their assumed LUMO at +2.09 eV, they have identified (but ignored) another peak at about 1.0 eV, as they mention in their supporting information. If, in line with the previous assumptions, this peak is adopted as the real LUMO, then the "renormalized" gap would be about 1.69 eV, very close to the "real gap" and to the Kimouche et al. [4] "corrected" band gap. Then the conclusions drawn from our data and the seemingly conflicting STS data, based on our current assump-

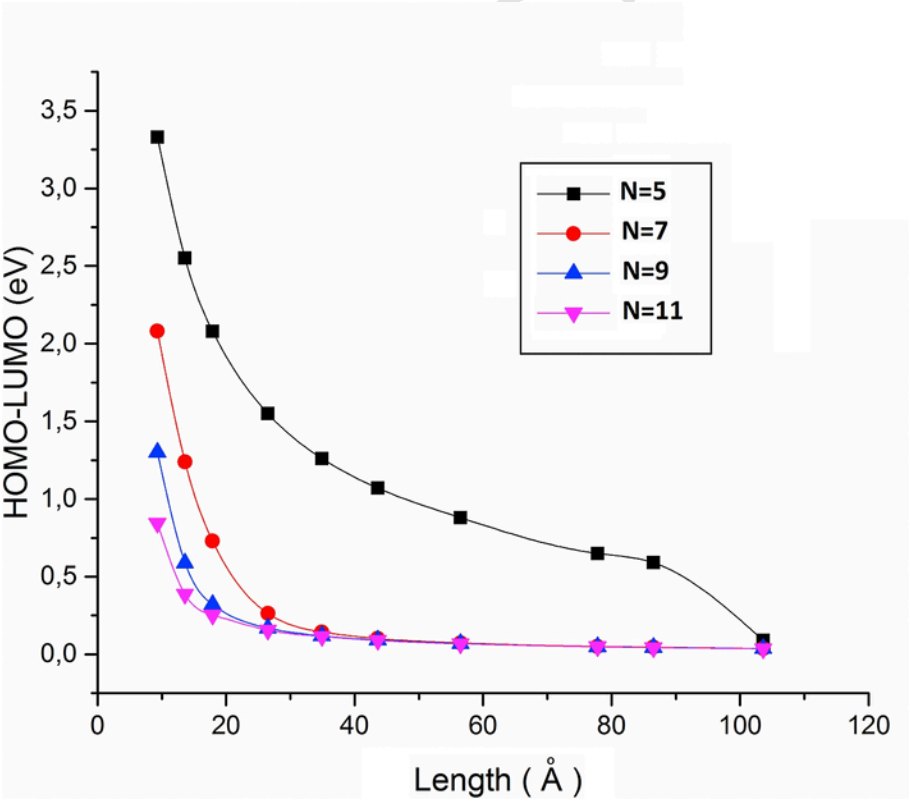

Fig. 5. Length dependence of the HOMO-LUMO (DFT/PBE0) gap of representative GNRs with constant widths N = 5, 7, 9, and 11. (A colour version of this figure can be viewed online.)

tions and speculations, should be that both measurements are compatible to each other and our own results (and in particular the excitation spectrum in Fig. 2). This is a very attractive outlook which we cannot ignore. If that is the case, we can further assume that the average length of the AGNRs in Zhang et al. [3] should be dominated by the three perylene monomers AGNR (3), which is statistically much more abundant than the rest.

2.2.1.2. The five perylene monomers (5) AGNR

For the 5 perylene monomers AGNR (5), Kimouche et al. [4] have assigned the HOMO-1, HOMO, LUMO, LUMO+1, LUMO+2, and LUMO+3: at −0.55 eV, +0.026 eV, 0.25 eV, 0.81, eV, 1.25 eV, and 1.57 eV respectively. The gap according to these assignments would be about 0.22 eV in clear disagreement with our TDDFT/PBE0 results which yield a gap of 1.03 eV (and HOMO-LUMO gap 1.07 eV) clearly assigned to the HOMO → LUMO transition with oscillator strength of 4.8027. If we assume that the samples are electrically neutral and exclude strong interactions from the Au substrate (which is a usual [3,4] and well documented [8] assumption), we are lead to suggest as a best possible combination to reconcile these data, the transition between the assumed LUMO and LUMO+2; leading to a gap of (1.25 eV-0.25) eV = 1.0 eV. If this is a valid assumption then the HOMO and HOMO-1 peaks (together with the LUMO+1) would be possibly associated with other transitions. This is a rather strong assumption. However, the about 1 eV gap for this AGNR is in full harmony with the continuous full gap variation curve of Fig. 4, from small up to much larger lengths.

2.3. The N = 7 AGNR

For this ribbon there are at least four experimental measurements [3,5–7]. and all of them seem to agree to each other for a gap of 2.5 ± 0.2 eV (2.3, 2.5, and 2.7 eV), in full agreement to our own gap prediction. As a matter of fact even the small variations (2.3 eV, 2.5 eV and 2.7 eV), which are well within experimental error, can be readily explained on the basis of our results, as due to AGNRs with different lengths. Thus, for N = 7 there is no apparent conflict neither between different experimental data, nor between experiments and our theoretical results. However, there is a large difference between our results and the theoretical results based in LDA + GW, which predict a gap of 3.8 eV, according to Table 1. Attempts to bridge this gap (difference), based on substrate-induced polarization effects (as in Ref. [5] for example) will be discussed below in section 2.6. Let us first concentrate in our present approach, which is based on the common prevailing assumption [6] that such polarization effects (on the gap) should be small even negligible [8]. As we can see in Fig. 5, the HOMO-LUMO gap at 56 Å, is in the saturation region with a magnitude of 0.07 eV. Yet the "effective HOMO-LUMO gap" [19] which is defined to avoid the edge zigzag effects (in our previous work [19]), consisting of the (LUMO+1)-(HOMO-1) energy difference, is 2.76 eV. As we can see in Fig. 1 (for the N = 7 GNR, and others), both HOMO and LUMO orbitals are strongly localized at the zigzag edges, in contrast to the "nearby" HOMO-1 and LUMO+1. At a larger length around 88 Å the HOMO-LUMO gap practically remains the same (0.065 eV) and similarly the "effective HOMO-LUMO gap" becomes 2.70 eV, in very good agreement with the measured gaps [3,5–7] of 2.5 ± 0.2 eV. The notion of the "effective gap" (or the energy separation of the effective HOMO, LUMO orbitals: HOMO*, LUMO*) was introduced in our previous work for graphene and graphene dots and antidots [19] in order to project to the infinite systems, by avoiding edge effects, which are associated with finite size. However, due to the finite size of the bottom-up synthesized atomically precise AGNRs, such size effects (with the exception perhaps of the short N = 5 AGNRs, in Fig. 3) are there and they are very important, as can be seen in Fig. 1 (see also the local density of states, LDOS, in Ref. [6]), since they dominate the wave functions at band edges, i.e. the HOMO and LUMO orbitals. However, due to the massive "concentration" of the electron density in the wave functions of HOMO and LUMO at the zigzag edges, these orbitals have very low overlaps and, as a result, the transitions between HOMO and LUMO (or the STS peaks which are dominated by transitions from HOMO to LUMO) would be very weak and practically undetectable by STS. Thus, on the basis of Fig. 1, the STS gap would be determined (or dominated) by the HOMO-1 and LUMO+1 orbitals. In the one electron (one body) approximation, the STS gap for the AGNRs of Fig. 1 would correspond to the (HOMO-1)-(LUMO+1) effective gap. Thus, the STS gap would be expected to be always larger or equal (only in special cases of spatially extended HOMO and LUMO orbitals as in the short N = AGNRs) to the optical gap, which is determined by the real (not the effective) HOMOs and LUMOs. Due to the high orbital overlaps the transition corresponding to the STS would have a large intensity and would correspond to a large oscillator strength transition in the excitation spectrum. In Fig. 6 we show our calculated "many body" TDDFT excitation spectrum of a representative N = 7 AGNR of length about 5.6 nm (56 Å), which is well in the saturation region and in the experimental range of the samples (3–11 nm) [6]. As we can see in Fig. 6, the strongest peak is located at 2.3 eV in excellent agreement with the results of Ruffieux et al. [5] (2.3 eV) and of Refs. [3,5–7] (2.5 ± 0.2 eV). According to our earlier discussion, this 2.3 eV peak, which has been identified (in four different works) as the real band gap, is indeed the real STS gap and corresponds to an intense excitation with a relatively high oscillator strength (2.6958) which is dominated (83%) by the HOMO-1 to LUMO+1 transition, in which both end- orbitals, as we can see in Fig. 1 (7), are non-edge states, corresponding to the effective HOMO, LUMO orbitals. The one-electron STS effective gap (HOMO*-LUMO*) is 2.7 eV for this AGNR. This explains the success of the effective HOMO-LUMO gap in relevant comparisons (see also the discussion for the N = 13 AGNR and the associated figure).

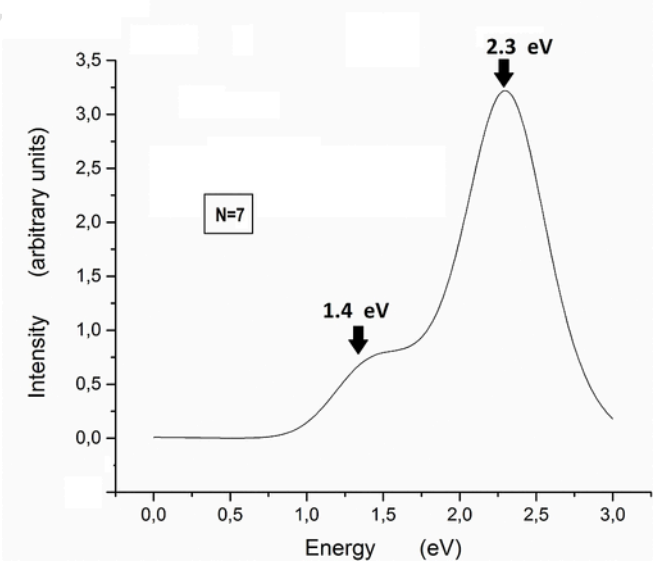

Fig. 6. The many-body TDDFT/PBE0 excitation spectrum for the N = 7 AGNR of width 9.2 Å and length 56.5 Å. The vertical arrows indicate the primary peak at 2.3eV and a secondary "shoulder" at 1.4 eV.

Moreover, in the spectrum of Fig. 6 we can also observe a weaker (relative oscillator strength 0.62/2.7) peak (or "shoulder") at 1.4 eV, which is dominated by the HOMO to LUMO+2 (65%) and HOMO-2 to LUMO (33%) transitions, involving as one of the two end-orbitals either the HOMO or the LUMO, which are edge localized. The direct HOMO to LUMO transition corresponds to the first excited state located at 0.024 eV (close to the HOMO-LUMO gap of 0.07 eV), and is characterized by a non-zero but extremely small (0.009) oscillator strength. Technically speaking this excitation defines the optical gap, if we stick to the definition of the optical gap as the energy of the lowest allowed excitation (with non-zero oscillator strength) [14,15]. However, in practice for a transition to appear in the (optical) spectrum the oscillator strength must be "appreciable", a term which is very much dependent on the experimental conditions and the level of theoretical treatment. In this respect the secondary peak at 1.4 eV, dominated by (linear combination of) transitions between spatially extended and edge- localized orbitals could be assumed to define an "extended" optical gap". Obviously, transitions between orbitals which are both spatially extended (such as the HOMO-1 and LUMO+1 in Fig. 1) would correspond to much stronger peaks, but would be located energetically higher. This is exactly the case for the 2.3 eV peak, defining the STS gap in the spectrum of Fig. 6, which, as we have seen above, is dominated (83%) by the HOMO-1 to LUMO+1 transition and corresponds to relatively high oscillator strength (2.6958). Thus, we can see that the size of the STS gap, which is "responsible" for the first kind of discrepancies, is directly related to the electron distribution in HOMO and LUMO, which is responsible for the second kind of ambiguities. We can therefore identify the optical gap as the energy of the lowest excitation with non-zero or "appreciable" oscillator strength and the STS gap as the energy of the lowest excitation with "large" oscillator strength. On the basis of our experience with the current work we could venture to arbitrarily assign some typical oscillator strength values to loosely characterize (or distinguish) the "regions" of optical and STS gaps. To facilitate such comparisons for the current samples we could suggest a lower limit of 0.1 (appreciable) for the "critical oscillator strength" for the optical gap; and the larger value of 1.0 for the "larger" STS gap. Although the selections rules are not expected to be the same for STS and optical (UV) spectroscopy, it is clear from the up to now results and discussion that the (strongest) peaks appearing in STS correspond to the strongest peaks in the excitation (absorption) spectrum. Thus, the 1.4 eV peak (involving transitions with one edge-localized and one delocalized frontier orbitals), which is characterized by an oscillator strength of 0.62, does not appear in none of the experimental STS data. It is interesting to observe, however, that a peak of about the same energy but of much higher oscillator strength defines the STS gap of the N = 13 AGNR which belongs to same family of N = 3p+1 (p integer) with N = 7 AGNR (see discussion below).

2.4. The N = 9 and N = 11 AGNRs

We are not aware of any STM/STS experimental data for the N = 9 and N = 11 AGNRs. Thus, our results for these AGNRs are theoretical predictions to be compared at the moment only with the LDA and LDA + GW, which are shown in Table 1, and Table 3. These values correspond to lengths around 10 nm (10.34). At half this length (5.64 nm) the corresponding (STS) gaps for these AGNRs are 1.55 eV and 0.73 eV respectively.

Table 3
Theoretical Results for the N = 9 and N = 11 AGNRs, including HOMO-LUMO gaps (H-L), effective HOMO-LUMO gaps (H*-L*) and TDDFT band gaps (E_g) in comparison to the LDA and LDA + GW results of Yang et al. [10].

	H-L (eV)	H*-L* (eV)	E_g (eV)	LDA (eV)	LDA + GW (eV)
N = 9	0.04	**1.75**	**1.6**	0.7	2.0
N = 11	0.04	0.45	**0.45**	0.2	0.9

2.5. The N = 13 AGNR

On the basis of the discussion for the N = 7 AGNR, it is clear that we can have a quick and "inexpensive" evaluation of the gap by looking at the morphology of its frontier orbitals. As we have seen in the case of the N = 7 AGNR, the TDDFT STS band gap corresponds to an intense excitation with a relatively high oscillator strength and is dominated by the HOMO-1 to LUMO+1 transition, in which both end-orbitals of the transition, as we can see in Fig. 1 (7), are non-edge states. Such states determine what we have earlier (in this and previous [19] work) defined as effective HOMO, LUMO orbitals and the effective (STS) gap. In this respect, the transition from the HOMO* (usually the HOMO-1) to the LUMO* (usually the LUMO+1) orbitals, which are characterized by "large and wide" electron distributions, would be expected to have large oscillator strength (intensity). This is clearly true for the N = 7, 9, and 11 cases examined here. For the N = 13 AGNR not only the HOMO and LUMO are zigzag edge-localized (as shown in Fig. 1), but also the HOMO-1, and in part the LUMO+1 (and certainly the LUMO), as shown in Fig. 7. In full agreement with the experimental LDOS of Chen et al. [6], Fig. 7, reveals conduction and valence band edge states which are strongly localized along the edges of the ribbon. Furthermore, this figure is in extraordinary agreement with the measurements of Chen et al. [6] who have observed localized states that can extend up to 30 Å into the ribbons, and they have unambiguously identified and associated such "end states" with the zigzag edges. From Fig. 7 we can easily see that the effective HOMO* orbital in this case would be the HOMO-2 orbital. However, the effective LUMO* could be either the real LUMO, which we have adopted here, or (with very small energy difference) the LUMO+1, or even the LUMO+2 orbital, which is clearly "bulk-like" (but at higher energy).

In the first (and simplest) case the STS gap would be about 1.4 eV in full agreement with the experimental results of Chen et al. [6] and the calculated excitation spectrum shown in Fig. 8.

This is because, in contrast to the HOMO and HOMO-1 orbitals which are fully localized, and the LUMO and LUMO+1 orbitals which are partially localized at the ribbon zigzag edges, the HOMO-2 is clearly non-edge orbital, extended throughout the main body of the ribbon. Indeed, the TDDFT results verify that the primary peak is located at 1.35 eV and (as was expected on the basis of Fig. 7) is dominated (by 92%) by the HOMO-2 to LUMO transition and only 4% by the HOMO-4 →LUMO+1 transition. The same HOMO-4 →LUMO+1 transition contributes more than 87% in the "shoulder" in the TDDFT spectrum of Fig. 8 at about 0.4 eV above the primary peak (1.75 eV), with intensity (oscillator strength) almost 1/3 of the main peak. Such a "shoulder" has been clearly observed by Chen et al. [6] At first sight it is rather surprising that such observed shoulder involves the HOMO-4 → LUMO+1 transition instead, let's say, the HOMO-3, which is energetically closer. This can be understood however by a closer examination of the morphology of the involved orbitals in Fig. 7. As we can see in Fig. 7, The HOMO-4 orbital extends further to the zigzag edges of the GNR (compared to the HOMO-3) and as a result it has a much higher overlap with the LUMO+1 or-

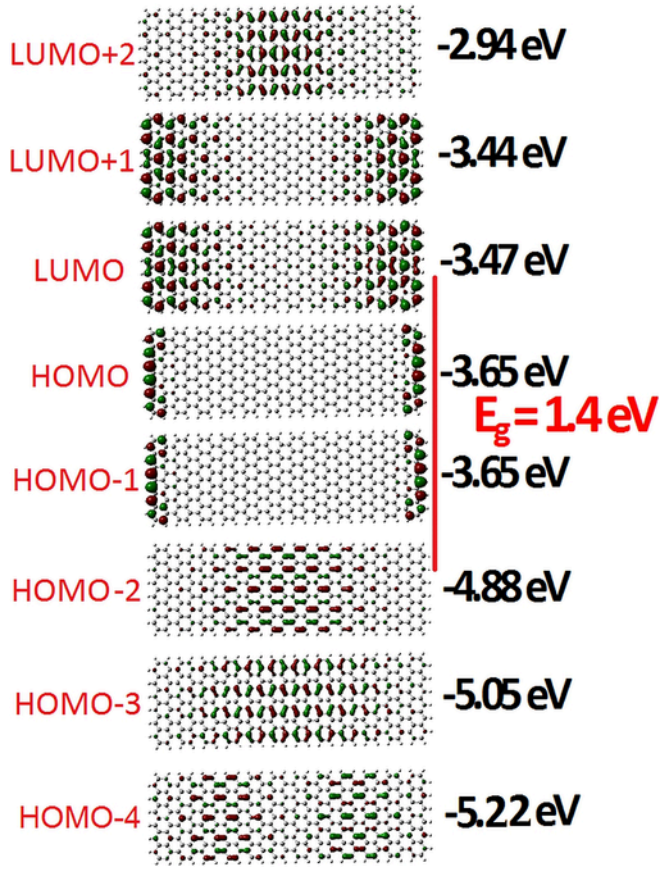

Fig. 7. The frontier orbitals of the N = 13 AGNR with length (including the end hydrogens) 5.7 nm. The vertical red line indicates the proposed HOMO* - LUMO* gap [19] of about 1.4 eV. The black line at the left side of the figure indicates the transition between orbitals of maximum overlap. (A colour version of this figure can be viewed online.)

bital. The HOMO-3 →LUMO+1 transition is energetically located at about 1.55 eV, but is more than 10 times weaker and therefore is not observable. At the lower energy part of the spectrum we have found a weak but prominent "shoulder" at 0.23 eV, which is a "midgap" state corresponding to a linear combination of HOMO-1 → LUMO (60%) and HOMO→LUMO+1 (37%), which are (fully and partially) edge-localized. This is in excellent agreement with the experimental findings and characterization of Chen et al. [6] who have found (and fully characterized) an "end state" at (0.20 ± 0.2) eV. Furthermore, Chen et al. [6] have clearly illustrated that the magnitude (intensity) of shoulders and prominent peaks, especially of the empty states, depends on the position of the STM tip within the GNR, and on its condition. This could clearly explain some of the experimental discrepancies and uncertainties. These results have been derived for the N = 13 AGNR with length about 4.4 nm. At 6.1 nm length the TDDFT gap shifts to 1.17 eV, still in very good agreement with experiment (STS).

2.6. The effect of the gold substrate

2.6.1. Working assumptions and possible pitfalls

As we have illustrated in the previous sections, the simple and transparent (by choice) real space method we have employed, based on DFT/PBE0 and TDDFT/PBE0 (using the hybrid PBE0 functional) was very efficient and successful in reproducing and predicting the energy gaps of the atomically precise AGNRs we have examined in this work. The same technique (DFT/PBE0) was also very successful in reproducing earlier [19,20] the aromatic and electronic (bonding and banding) properties of graphene and several graphene-based structures (dots and antidots) [19,20], as well as the electronic, ground state (DFT) and excited state (TDDFT) properties of perylene (see Table 2). The combination of TDDFT involving hybrid functional is known to be very successful for the excitation spectrum of relatively large nanostructures [14,15]. Recently such calculations for silicon nanocrystals [21] were very successful in reproducing very accurately the optical gaps of Si nanocrystals in a large size range all the way to the infinite Si crystal. Thus, such real-space methodology, starting from aromatic hydrocarbons and "molecules" or "nanocrystals" all the way to infinite structures, following a "chemical description" (in contrast to k-space or band structure description which constitutes a "physical methodology"), can be thought as "bridging Chemistry and Physics" [22]. For large enough ("infinite") materials the band theory was traditionally used. However, for graphene nanostructures, which have been recently become one of the central issues in carbon science, the band theory cannot allow a comprehensive description [22,23], due to the smallness in size and the edge effect(s). This is the central issue of this work, which (as in every theoretical work), besides the fundamental (mean field, DFT, adiabatic) approximations which define the "level of theory", involves further (simplifying) assumptions and technical approximations.

For example, the results presented here for the AGNRs were clearly derived for free-standing AGNRs, but they were applied to (and compared with) AGNRs supported on Au(111) surface, following (tacitly) the prevailing assumption [6] that the Au substrate has marginal or negligible [8] effect on the gap. Another assumption underlying the results and conclusions presented here is the connection and interrelation of the STS (HOMO-LUMO) and the optical gap. Both of these assumptions have been challenged by Ruffieux et al. [5] who have adopted the large (3.8 eV) LDA + GW gap [10] for free-standing N = 7 AGNRs (independent of length) and assigned the 1.5 eV difference of the measured gap to the gold substrate polarization-induced corrections, without taking into account neither the finite length of the atomically precise N = 7 AGNR, nor the zigzag edge localized band edges [6] (as in Figs. 1 and 7). Furthermore, according to Ref. [5], no relation exists whatsoever between optical gap and STS gap. However, in a later work [24] from the same group it was concluded that the optical gap and STS gap for the N = 7 AGNRs are of equal magnitude (2.1 eV and 2.3 eV respectively). The difference of 0.2 eV between the two is well within the error margin due to experimental uncertainties and the theoretical (and experimental) differences for different lengths. Therefore, the two (optical and STS) gaps for the N = 7 AGNRs are "equal" (accidentally, due to cancelations, according to Ref. [24]). Yet, the same (approximate) equality for STS [6] and optical gaps we have found also for the N = 13 AGNR, as was illustrated above in section 2.5. Can we consider this equality accidental as well? Perhaps one could; although in this case, such "accident" would be very "systematic", since in (only) two known cases we have in both of them the same "accident". Even then, one can calculate one of the two gaps (obviously the one that is calculated in the simplest, more economical and transparent way) and determine the other one with accuracy of about 0.1 eV. In such a case, we can stick to the (finite size) DFT/TDDFT results (as in the present work) and assume (as in several works before) that the effects due to the gold substrate are either small or cancel out, at least for the lengths and widths examined here. There is no doubt that the presence of the metallic substrate implies that there is an image charge density in addition to the one we already have for free standing AGNR. This additional image charge (IC) density has opposite sign from the free standing AGNR and induces a polarization which leads to a (renor-

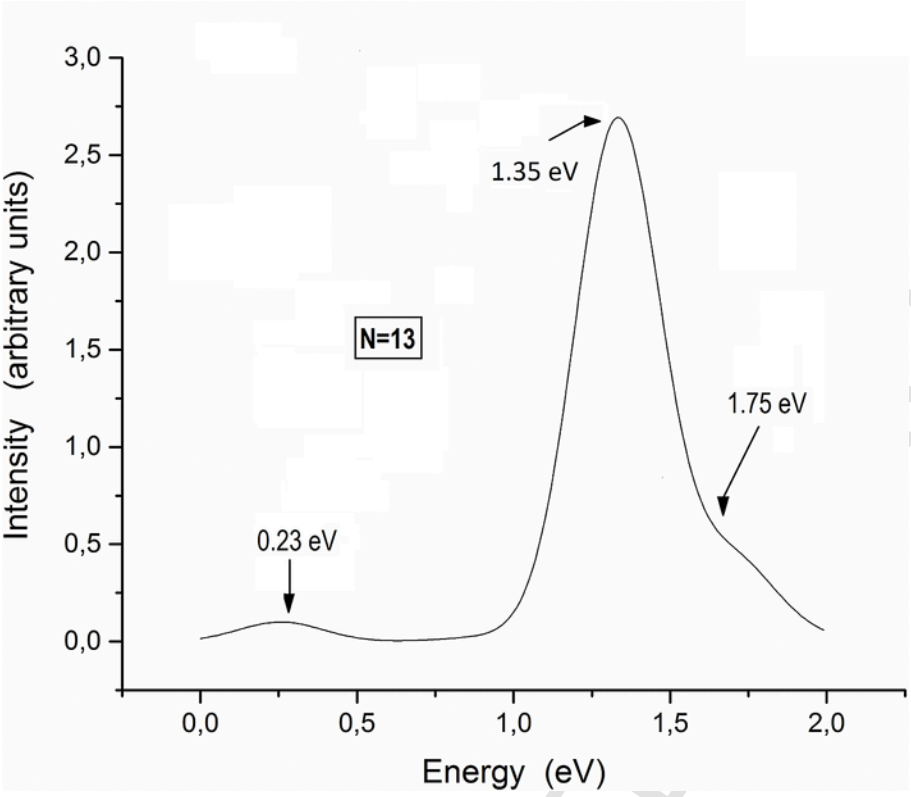

Fig. 8. The excitation spectrum of the N = 13 AGNR of width 16.7 Å and length about 57 Å (including the end hydrogens).

malized) lower gap due to the presence of the metallic substrate [24–29].

However, the real question is the actual magnitude of the IC corrections. For instance, since the real reference point is the magnitude of the experimental STS gap (with or without any possible uncertainties), if a theoretical treatment overestimates (or underestimates) the primary (free-standing) gap, then the same methodology could equally well overestimate (or underestimate) the IC corrections, thus possibly leading to a fictitious agreement with experiment. A very simple example of this is provided by the PBE results in Table 2 for pelylene (monomer and polymers) by comparing the calculated HOMO-LUMO and optical gaps (which are directly measurable). The non-hybrid PBE functional substantially underestimates the one-particle (HOMO-LUMO) gap(s). The "many-body" TDDFT correction clearly improves the gaps (in comparison to the measured values), but overemphasizes the "many body" corrections (4 times larger compared to the PBE0 values). Thus, according to the PBE0, which gives much better agreement with experiment (99.3% for perylene), the many body corrections of the gap are slightly less than 10%. In contrast, the PBE functional (with much less accuracy 87%) yields an almost 40% many-body correction for the gap (4 times larger), which is unrealistic, especially in view of the resulting negative quasiparticle binding energy. Thus, the magnitude of the "corrections" very much depends on the zeroth order values, and, obviously, the method of calculation for both of them.

As mentioned before, every theoretical approach consists of a (self-consistent) set of approximations, assumptions, and idealizations, which should be fully consistent to each other and should, obviously, grasp the essential features of the problem. Then, the "renormalized" question could be: What is more important of the two (if one has to choose only one), the finite length and the zigzag edge localization of the band edges, or the IC corrections? This is a question which could be explored within our present (simple, transparent, efficient, and wide-spread) approach. We fully and directly address this problem in the next section 2.6.2. The GW approach, however (clearly more advanced, than DFT/PBE0), is very much computationally demanding (and non-transparent). Thus, IC corrections are taken afterwards into account indirectly and approximately [5,24–29], usually by considering the classical image charge potential (reduced to[24] 1/4z for r = r', where z is the vertical distance of the AGNR from the metallic substrate) in the HOMO and LUMO charge density matrix elements. This correction depends on the screening length and the vertical distance z of the AGNR from the metallic substrate. Ruffieux et al. [5] have used a screening length of about 30 Å (too large, we believe) and z = 3.15 Å. For this value of z and a screening length of 30 Å, one would expect on the basis of simple scaling arguments a gap reduction of about $(a/2z)\exp(-6.3/30) \sim 18\%$, where a = 1.42 Å is the nearest neighbour distance in graphene. If z is larger than 3.15 Å the gap reduction (renormalization) would be smaller. If z gets small (smaller than the real equilibrium distance) we could still get a much smaller gap renormalization. However, Khomyakov et al. [25] have shown that if the distance becomes "too close" the opposite effect, i.e. bang-gap opening, could happen due to hybridization of the Au d with AGNRs p_z orbitals. Obviously, such an effect could possibly cancel the band-gap lowering due to polarization from the image charge. Another possible pitfall of the IC model has been pointed out by Denk et al. [24] in their work on the STS and excitation spectrum of the N = 7 AGNR. We quote from the supporting information of Denk et al.[24]: "Note that the extended nature of the studied systems raises further questions regarding the application of the IC model. In fact, if the charge to be added/removed from the system is connected to an extended Bloch state instead of a localized molecular orbital, the

charge density that needs to be screened by the surface is infinitesimally small, thus leading to a negligible correction". Most of these subtle points we will illustrated below in a simple and transparent example.

2.6.2. A simple and transparent model for the N = 5 (2 × 6) AGNR @ Au(111)

In this section we examine the N = 5 AGNR consisting of three perylene monomers (2 × 6), $C_{60}H_{28}$, which we have considered in detail in sections 2.1 and 2.2 (and Table 2). This choice stems from fundamental and practical reasoning. Firstly, although there exist two independent studies [3,4] for this AGNR(s), and despite the detail experimental (and theoretical) study of this particular (3 perylene monomers) AGNR, there are not any IC calculations, to our knowledge, in the literature, contrary to the N = 7 and (lately [27]) N = 13 AGNRs. Secondly, since this (2 × 6) AGNR is of small size (length and width), it is much easier to model (in real space) the combined $C_{60}H_{28}$@Au(111) system, especially if we want to examine a variety of geometries. Finally, according to Table 1, the IC corrections required to bridge the discrepancies between theoretical LDA + GW and experimental values would be the largest (more than 90%) from all AGNRs examined here. In Fig. 9 we illustrate the morphology of the "band edges", i.e. the HOMO and LUMO orbitals in the free-standing and the Au(111) supported geometries.

The height z of the AGNR from the topmost Au(111) layer is taken z = 3.54 Å for the PBE0 results, corresponding to the maximum of the binding (or interaction) energy E_b between the AGNR and the gold substrate calculated with the PBE0 functional:

$$E_b(\text{AGNR, Au}) = E(\text{AGNR}) + E(\text{Au}) - E(\text{AGNR@Au}), \quad (1)$$

where E(AGNR) and E(Au) are the total energies of the individual AGNR and Au respectively and E(AGNR@Au) is the total energy of the combined system.

If we divide this energy (at the maximum) by the number of carbon atoms (here 60) we get the binding energy per carbon atom equal to 0.025 eV/atom, at the theoretical level of DFT/PBE0. This energy corresponds to the energy per carbon atom required to remove the AGNR sheet from the metal substrate. The corresponding value for graphene, which has a maximum binding energy at 3.31 Å, according to Khomyakov et al. [25] is 0.03 eV/atom, fully consistent with our results in Fig. 9 which have been obtained for drastically truncated Au(111) geometries, consisting of one and two Au(111) sheets, restricted to 58 and 150 Au atoms respectively at the bulk geometry in the neighbourhood around and below the AGNR. This is highly suggestive that this very simplified model, in which the image potential is naturally and a priori included in the Hamiltonian (and the corresponding charge density), contains the essential ingredients of the problem. We will find further evidence for this below. By drawing now the orbitals of the combined AGNR@Au system, in an appropriate energy window around the Fermi level, we can identify in a simple and straightforward way the effective AGNR HOMO and LUMO orbitals ("HOMO" and "LUMO", respectively) and from their energy separation, as shown in Fig. 9, the renormalized HOMO-LUMO gap. From the PBE0 results (in the central portion of the figure) we can see that the renormalized gap of 2 × 6 AGNR at the equilibrium height z = 3.54 Å is 1.43 eV, a reduction of 0.13 eV or 8.33% from the primary gap of 1.56 eV. From Fig. 9 we can see that the same reduction of 0.13 eV is also obtained for the PBE functional (known to underestimate the gap). However, due to the underestimation of the primary gap, this corresponds to a larger percentage (18.6%) in reduction. It should be emphasized that the equilibrium height that we have calculated with the PBE functional including also empirical dispersion corrections [30] (see methods) is z = 3.15 Å, identical with the one obtained by Ruffieux et al. [5] using much larger Au(111) slab, containing 5 layers, and a similar to the LDA-like PBE, (DFT/LDA) functional. This is an additional testimonial that this simple model contains indeed all or most of the essential physics and chemistry of the problem. This is also verified by the fact that the larger model, with two layers of Au, gives practically the same renormalized gap (0.59 eV versus 0.57 eV) at the same height z. Furthermore, as we can see in Fig. 10 (a), the variation of the renormalized gap with the height z is in full accord with the results of Khomyakov et al. [25] showing that at very short heights (here shorter than 3.48 Å, according to Fig. 10(a)) instead of band-gap reduction we could have bang-gap opening, due to hybridization of the Au d with AGNRs p_z orbitals (see also Fig. 11 below). Clearly, according to the present results, the equilibrium height obtained with the PBE functional z = 3.15 Å is within the region of hybridization, for which the IC model is strictly not valid. Thus, the use of this functional could be a source of a rather large error (in the interpretation of the data). We can clearly see in Fig. 10 (b) that at the DFT/PBE0 equilibrium height z = 3.54 Å the PBE IC correction is zero.

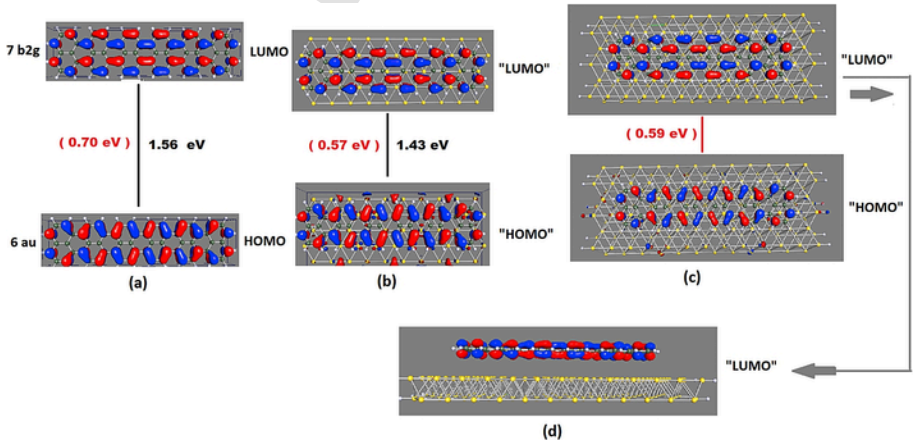

Fig. 9. Morphology of the wave function at the band edges: (a) for the free standing (HOMO, LUMO); and for the 1 and 2-layers Au(111)- supported, (b) and (c), 2 × 6 N = 5 AGNR ("HOMO", "LUMO"). The "LUMO" orbital in (c) is also shown in a side view in (d). The numbers next to the vertical lines indicate the energy gaps obtained with PBE0 (black color) and PBE (red color, in parenthesis) functionals respectively, at their calculated equilibrium distances. (A colour version of this figure can be viewed online.)

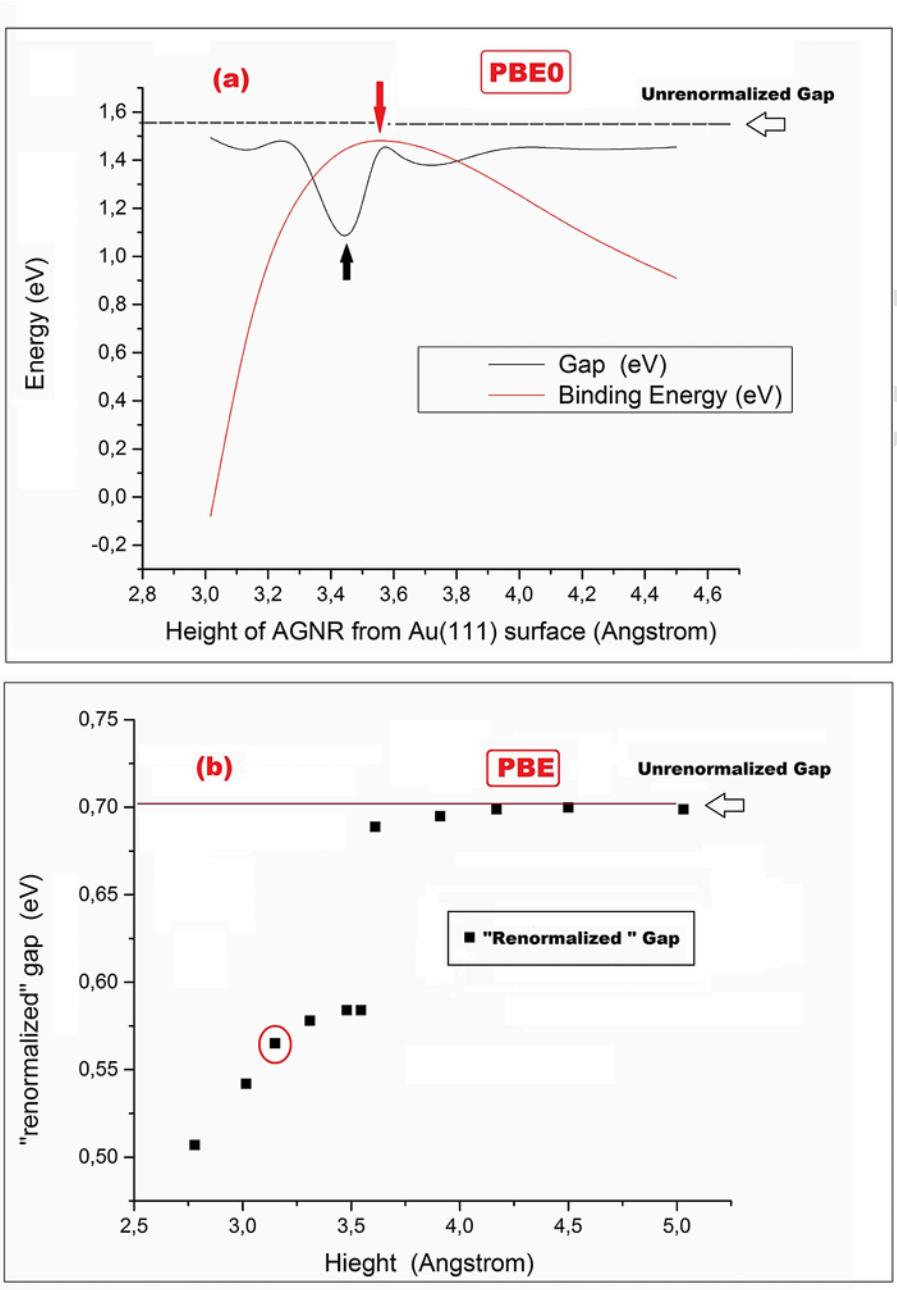

Fig. 10. Variation of the renormalized DFT band-gap with the height z of the AGNR from topmost layer of the Au(111) substrate obtained with the PBE0 (a), and the PBE (b) DFT functionals. In (a) the variation of the binding energy E_b of eq. (1) is shown as well. The vertical arrows mark the maximum of the binding energy (red), and the minimum of the renormalized gap, according to the DFT/PBE0 calculations. The red circle in (b) shows the point of minimum renormalized gap according to PBE functional. (A colour version of this figure can be viewed online.)

In Fig. 11, we show the successive transformations of the effective "LUMO" orbital of Fig. 9, at z = 3.54 Å, in terms of z, from Au(111)-like for z = 4.10 to fully $C_{60}H_{28}$-like at z = 3.91 Å (and 3.54 Å), and, finally, to mixed Au(111)+ $C_{60}H_{28}$-like (hybridized) at 3.15 Å, in full accord with the conclusions of Khomyakov et al. [25] and our results in Figs. 9 and 10. Thus, our results from this simple and transparent (by choice) model are "self-consistent" and fully consistent with the known results in the literature [24–26]. This is highly suggestive that our approach (at least for such finite and "short" N = 5 AGNR) is essentially correct and efficient.

Thus, the IC correction in this case should be clearly considered negligible. An IC correction of 0.13 eV (8%) would practically make no difference whatsoever, especially in view of much larger uncertainties (more than 1 eV) in the literature. However, one could possibly argue that the "short" N = 5 AGNR is a "special case". After all, if the theoretical (LDA + GW)-experimental [4] discrepancy (1.6 eV, see Table 1) for this (N = 5) AGNR was solely due to substrate IC corrections, such corrections would have to be more than 90% (or more than 1500% of the measured value). Clearly, we cannot exclude such "special-case" possibility, although we believe that IC correc-

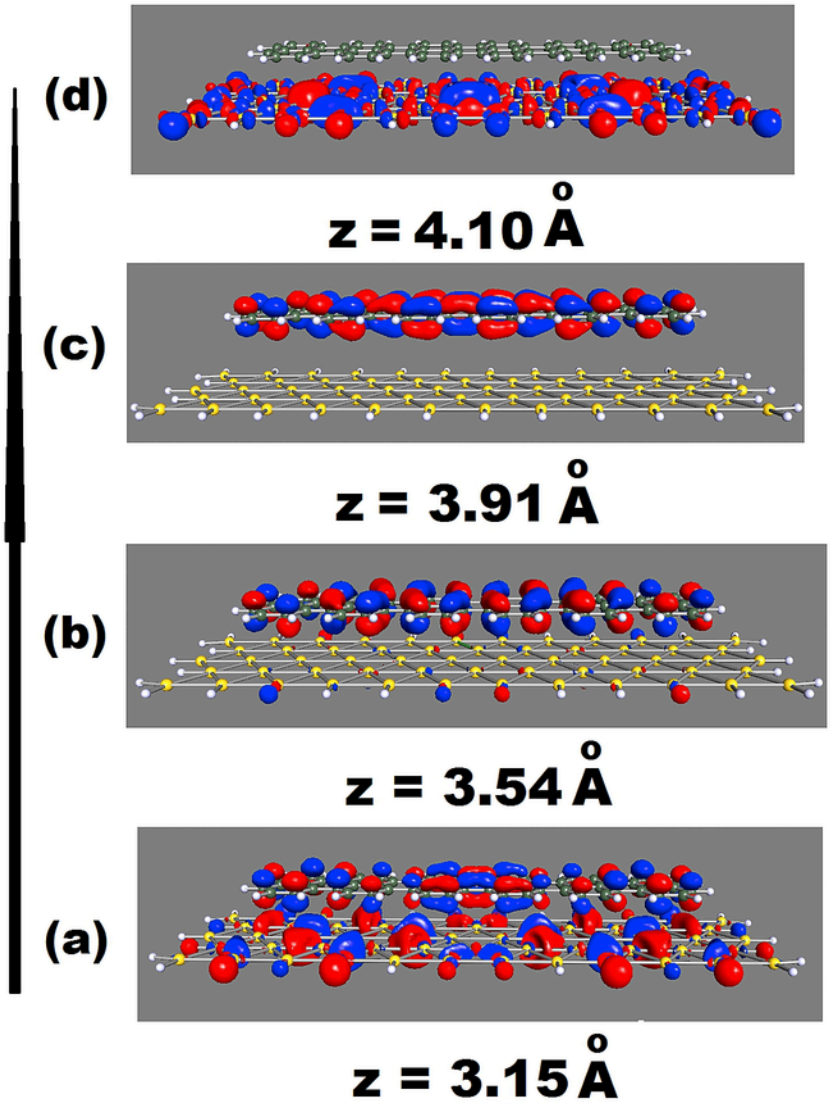

Fig. 11. The effective "LUMO" orbital of Fig. 9 for the $C_{60}H_{28}$@Au(111) system at various heights of the $C_{60}H_{28}$ AGNR above the Au(111) surface. (A colour version of this figure can be viewed online.)

tions of the order of 40% or 50%, for the other AGNRs examined here are highly improbable as we have explained earlier.

In all this discussion, we have considered only the HOMO-LUMO gaps, and not gaps obtained from the excitation spectrum (optical gaps) calculated by TDDFT, for two fundamental reasons: First, as was explained before, the excitation spectrum and the corresponding gaps are affected much less (or not at all) compared to the HOMO-LUMO gaps [26], for reasons we have explained before. Second, for this particular AGNR, as can be clearly seen in Table 2 and Fig. 4, the HOMO-LUMO and the "many-body", optical gaps practically coincide.

3. Conclusions

We have successfully invoked a theoretical and computational framework based on TDDFT, through which we can describe and reproduce (in a uniform and easily accessible way) all known experimental data on finite (relatively "short") atomically precise AGNRs; and predict the key characteristics (STS gap and band-edge morphology) for the N = 9, 11 AGNRs for which not known (at least to present authors) experimental data exist up to now. We have also fruitfully studied the length dependence of the key characteristics of all AGNRS and have identified a semiconductor-metal transition with increasing length for the N = 5 AGNR. Moreover, we have clearly demonstrated that wherever experimental and/or theoretical discrepancies exist, as in the case of the very narrow N = 5 AGNRs, this is primarily due to the finite length of the samples in connection with experimental uncertainties in the determination of the STS gap, which, as we have illustrated, is always larger (or equal for N = 5) compared to the optical gap and corresponds to the lowest "stronger" transition (with large oscillator strength in the excitation spectrum). It is suggested that for finite ("short") AGNRs, the STS gaps which are calculated in this way, are not affected appreciable by the existing substrate-induced polarization corrections. As we have illustrated, such

effects, for such "molecular-like" atomically precise AGNRs (as the three perylene monomer N = 5AGNR), can be ignored (especially in comparison to other uncertainties), provided the STS gaps are calculated according to our suggested method (through TDDFT and/or "effective" HOMO*-LUMO* gaps). The ambiguities in the interpretation of the experimental data are largely due to the finite size (length) of the AGNRs and the resulting edge effects (localization of the frontier orbitals at the zigzag edges). The theoretical discrepancies, among others, are largely related with intrinsic problems, especially of the LDA-based DFT (non-hybrid) functionals.

4. Methods

All GNRs examined here, generated by suitably (and theoretically) cutting ribbons from large real space rectangular graphene models, such as the ones used in our previous work [19,20], were fully geometrically optimized by all electron DFT calculations using tight convergence criteria for forces and displacements, as implemented in the GAUSSIAN [31] program package, which was used for all free-standing calculations. The hybrid "advanced" PBE0 functional of Adamo et al. [17] was employed and the 6-31G(d) basis set was used, as incorporated in the above package, for all (small and large) structures. Occasionally, for smaller GNRs the results were tested with much larger, 6-311G(d,2p) basis sets without significant differences. The same package [31] was also used for the TDDFT/PBE0 single point calculations at the DFT/PBE0 optimized geometry. Such large scale TDDFT calculations (involving hybrid functional) for relatively large nanostructures have been done very recently for silicon nanocrystals by our group [21] very successfully, reproducing very well the known gaps of the Si nanocrystals all the way to the infinite crystals. The plots of the excitation spectrum were obtained by summation and Gaussian broadening (0.1 eV) of the excitation energies, weighted by the corresponding oscillator strengths. The largest part of the calculations of section 2.6 for the 2 × 6 AGNR supported on Au(111) were performed with the TURBOMOLE [32] program package using both PBE0 and PBE functional and the def2-SV(P) and def2-TZVP basis sets [33]. The PBE functional was used in conjunction with the "resolution of the identity" (RI) approximation [34,35], including empirical dispersion corrections [30]. To check the consistency of the results and their accuracy we have used in several cases both H-passivated and non-passivated Au(111) models, consisting of one and two layers and we have also applied two different basis sets. In all of these cases the influence on the final renormalized gap, due to the presence of the metallic substrate was marginal of the order of ±0.1 eV. The drawing of the orbitals for the TURBOMOLE runs was performed with the TmoleX program package [36].

Acknowledgment

This work was supported by the European Research Council under ERC Advanced Grant No. 320081 (PHOTOMETA), the Greek project ERC-02 EXEL (grant no. 6260), and under a grant by Air Force numbered 073037 FENIM.

References

[1] J. Cai, P. Ruffieux, R. Jaafar, M. Bier, T. Braun, S. Blankenburg, M. Muoth, A.P. Seitsonen, M. Saleh, X. Feng, et al., Atomically precise bottom-up fabrication of graphene nanoribbons, Nature 466 (2010) 470–473.
[2] Y. Segawa, H. Ito, K. Itami, Structurally uniform and atomically precise carbon nanostructures, Nat. Rev. Mater. 1 (2016). 15002–1-15002-14.
[3] H. Zhang, H. Lin, K. Sun, et al., On-surface synthesis of rylene-type graphene nanoribbons, J. Am. Chem. Soc. 137 (2015) 4022–4025.
[4] A. Kimouche, M.M. Ervasti, R. Drost, S. Halonen, A. Harju, P.M. Joensuu, J. Sainio, P. Liljeroth, Ultra-narrow metallic armchair graphene nanoribbons, Nat. Comm. 6 (10177) (2015) 1–6.
[5] P. Ruffieux, J. Cai, N.C. Plumb, L. Patthey, D. Prezzi, A. Ferretti, E. Molinari, X. Feng, K. Müllen, C.A. Pignedoli, et al., Electronic structure of atomically precise graphene nanoribbons, ACS Nano 6 (2012) 6930–6935.
[6] Y.-C. Chen, D.G. Oteyza, Z. Pedramrazi, C. Chen, F.R. Fischer, M.F. Crommie, Tuning the band gap of graphene nanoribbons synthesized from molecular precursors, ACS Nano (2013) 6123–6128.
[7] M. Koch, F. Ample, C. Joachim, L. Grill, Voltage-dependent conductance of a single graphene nanoribbon, Nat. Nanotechnol. 7 (2012) 713–717.
[8] A. Varykhalov, J. Sánchez-Barriga, A.M. Shikin, C. Biswas, E. Vescovo, A. Rybkin, D. Marchenko, O. Rader, Electronic and magnetic properties of quasi-freestanding graphene on Ni, Phys. Rev. Lett. 101 (2008) 15760.
[9] X. Yang, X. Dou, A. Rouhanipour, L. Zhi, H.J. Räder, K. Müllen, Two- dimensional graphene nanoribbons, J. Am. Chem. Soc. 130 (2008) 4216–4217.
[10] L. Yang, C.-H. Park, Y.-W. Son, M.L. Cohen, S.G. Louie, Quasiparticle energies and band gaps in graphene nanoribbons, Phys. Rev. Lett. 99 (2007) 186801.
[11] Y.-W. Son, M.L. Cohen, S.G. Louie, Energy gaps in graphene nanoribbons, Phys. Rev. Lett. 97 (2006) 216803.
[12] M. Ezawa, Peculiar width dependence of the electronic properties of carbon nanoribbons, Phys. Rev. B 73 (2006) 045432.
[13] O. Hod, J. Peralta, G. Scuseria, Edge effects in finite elongated graphene nanoribbons, Phys. Rev. B 76 (2007) 233401.
[14] A.D. Zdetsis, Optical properties of small size semiconductor nanocrystals and nanoclusters, Rev. Adv. Mater. Sci. (RAMS) 11 (2006) 56–78.
[15] C.S. Garoufalis, A.D. Zdetsis, S. Grimme, High level ab initio calculations of the optical gap of small Sillicon Quantum dots, Phys. Rev. Lett. 87 (2001) 276402.
[16] A.D. Zdetsis, The real structure of the Si_6 cluster, Phys. Rev. A 64 (2001) 23202.
[17] C. Adamo, V. Barone, Toward reliable density functional methods without adjustable parameters: the PBE0 model, J. Chem. Phys. 110 (1999) 6158–6169.
[18] T.M. Halasinski, J.L. Weisman, R. Ruiterkamp, T.J. Lee, F. Salama, M. Head-Gordon, Electronic absorption spectra of neutral perylene ($C_{20}H_{12}$), terrylene ($C_{30}H_{16}$), and quaterrylene ($C_{40}H_{20}$) and their positive and negative ions: Ne matrix-isolation spectroscopy and time-dependent density functional theory calculations, J. Phys. Chem. A 107 (2003) 3660–3669.
[19] A.D. Zdetsis, E.N. Economou, Is andidot functionalized graphene aromatic? unusual aromatic properties of graphene antidot lattices and antidot functionalized nanographens, J. Phys. Chem. C 120 (2016) 756–764.
[20] A.D. Zdetsis, E.N. Economou, A pedestrian approach to the aromaticity of graphene and nanographene: significance of Huckel's (4n+2)π Electron Rule, J. Phys. Chem. C 119 (2015) 16991–17003, http://dx.doi.org/10.1021/acs.jpcc.5b04311.
[21] S. Niaz, A.D. Zdetsis, Comprehensive ab initio study of electronic, optical, and cohesive properties of silicon quantum dots of various morphologies and sizes up to infinity, J. Phys. Chem. C (2016) 11288–11298, http://dx.doi.org/10.1021/acs.jpcc.6b02955.
[22] J. Zhang, M. Terrones, C.R. Park, R. Mukherjee, M. Monthioux, N. Koratkar, Y.S. Kim, R. Hurt, E. Frackowiak, T. Enoki, et al., Carbon science in 2016: status, challenges and perspectives, Carbon 98 (2016) 708–l732.
[23] S. Fujii, T. Enoki, Nanographene and graphene edges: electronic structure and nanofabrication, Acc. Chem. Res. (2013) 2202–2210.
[24] R. Denk, M. Hohage1, P. Zeppenfeld, J. Cai, C.A. Pignedoli, H. Söde, R. Fasel, X. Feng, K. Müllen, S. Wang, et al., Exciton-dominated optical response of ultra-narrow graphene nanoribbons, Nat. Comm. 5 (4250) (2015) 1–7.
[25] P.A. Khomyakov, G. Giovannetti, P.C. Rusu, G. Brocks, J. v. D. Brink, P.J. Kelly, First-principles study of the interaction and charge transfer between graphene and metals, Phys. Rev. B 79 (2009) 195425.
[26] J.M. Garcia-Lastra, K.S. Thygesen, Renormalization of optical excitations in molecules near a metal surface, Phys. Rev. Lett. 106 (2011) 187402.
[27] N. Kharche, V. Meunier, Width and crystal orientation dependent band gap renormalization in substrate-supported graphene nanoribbons, J. Phys. Chem. Lett. 7 (2016) 1526–1533.
[28] S. Wang, L. Talirz, C.A. Pignedoli, X. Feng, K. Müllen, R. Fasel, P. Ruffieux, Giant edge state splitting at atomically precise graphene zigzag edges, Nat. Comm. 7 (11507) (2016) 1–6.
[29] Yen-Chia Chen, Ting Cao, Chen Chen, Zahra Pedramrazi, Danny Haberer, D.G. Oteyza, F.R. Fischer, S.G. Louie, M.F. Crommie, Molecular bandgap engineering of bottom-up synthesized graphene nanoribbon heterojunctions, Nat. Nanotechnol. 10 (2015) 156–160.

[30] S. Grimme, Accurate description of van der Waals complexes by density functional theory including empirical corrections, J. Comp. Chem. 25 (2004) 1463–1473.
[31] M.J. Frisch, G.W. Trucks, H.B. Schlegel, G.E. Scuseria, et al., Gaussian 09, Revision C.01, Gaussian, Inc., Wallingford CT, 2009.
[32] TURBOMOLE (Version 5.6), University of Karlsruhe, 2000.
[33] F. Weigend, R. Ahlrichs, Balanced basis sets of split valence, triple zeta valence and quadruple zeta valence quality for H to Rn: design an assessment of accuracy, Phys. Chem. Chem. Phys. 7 (2005) 3297–3305.
[34] K. Eichkorn, O. Treutler, H. Oehm, M. Haeser, Auxiliary basis sets to approximate coulomb potentials, Chem. Phys. Lett. (1995) 283–290.
[35] F. Weigend, Accurate Coulomb-fitting basis sets for H to Rn, Phys. Chem. Chem. Phys. 8 (2006) 1057–1065.
[36] TmoleX, TmoleX a Graphical User Interface to the TURBOMOLE Quantum Chemistry Program Package, COSMOlogic GmbH & Co. KG, Imbacher Weg, 46, 51379 Leverkusen, Germany, 2015.